

Spin and Quadrupole Moment of  $I^{125}$  and the Magnetic Moment of  $I^{131}$ †

P. C. FLETCHER\* AND E. AMBLE‡

Physics Department, Columbia University, New York, New York

(Received October 7, 1957)

The spin and quadrupole moment of  $I^{125}$  have been determined by observations on the microwave absorption spectrum of  $CH_3I^{125}$ . Five absorption lines have been observed which fit the quadrupole hyperfine pattern of the  $J=2 \leftarrow 1$  rotational spectrum. The measurements indicate a spin of  $5/2$  and a quadrupole coupling constant of  $-2179 \pm 1$  Mc/sec. Using this and other known properties of the  $CH_3I$  molecule, the quadrupole moment of  $I^{125}$  is calculated to be  $-0.66 \times 10^{-24}$  cm<sup>2</sup>. This spin and quadrupole moment suggest a nuclear configuration for  $I^{125}$  similar to that of stable  $I^{127}$ , i.e., predominantly  $d_{5/2}$ . The magnetic moment of  $I^{131}$  has been measured by observation of the Zeeman splitting of the  $F=9/2 \leftarrow 9/2 (K=1)$  hyperfine line of the  $J=2 \leftarrow 1$  rotational spectrum of  $CH_3I^{131}$ . The magnetic moment is found to be  $2.56 \pm 0.12$  nuclear magnetons. The observations also confirm the previous results of Gordy *et al.* for the spin of  $I^{131}$  of  $3/2$  and quadrupole coupling constant,  $eqQ = -974 \pm 1$  Mc/sec. The magnetic moment measurement suggests a ground-state configuration similar to that of  $I^{129}$  which is predominantly  $g_{7/2}$  in nature but with large admixture of other states. The significance of these results are discussed.

## INTRODUCTION

FOLLOWING the microwave investigations on nuclear moments of the isotopic series of selenium<sup>1</sup> and chlorine,<sup>2</sup> work on the nuclear moments of iodine was begun. Besides the stable isotope,  $I^{127}$ , there are five radioactive isotopes with half-lives sufficiently long to be amenable to microwave spectroscopy;  $I^{124}$  with a half-life of four days,  $I^{125}$  with a half-life of sixty days,  $I^{126}$  with a half-life of thirteen days,  $I^{129}$  with a half-life of  $10^7$  years, and  $I^{131}$  with a half life of eight days. Of these, the spin and quadrupole moments of  $I^{127}$ ,<sup>3</sup> and  $I^{129}$ ,<sup>4</sup> and  $I^{131}$ ,<sup>5</sup> and the magnetic moments of  $I^{127}$ <sup>6</sup> and  $I^{129}$ <sup>6</sup> have been measured. In addition, the spin of  $I^{126}$  has been inferred from  $\beta$  radiations.<sup>7</sup> The magnetic moment of  $I^{131}$  has been determined here to give additional information about its ground state and to compare its value with  $I^{129}$  and other neighboring nuclei. The value measured,  $2.56 \pm 0.12$  nuclear magnetons, is only slightly smaller than that of  $I^{129}$ , indicating further that the ground state of  $I^{131}$  is similar to that of  $I^{129}$ . Because of the difference of configuration between  $I^{129}$  and  $I^{131}$  and the stable  $I^{127}$ , there is some interest in the spin and configuration of  $I^{125}$ . The results of this investigation, which gives the  $I^{125}$  nucleus a spin of  $5/2$  and a quadrupole moment of  $-0.66 \times 10^{-24}$  cm<sup>2</sup> (somewhat

larger than that of  $I^{127}$ ), indicates a predominantly  $d_{5/2}$  configuration for the  $I^{125}$  ground state.

## SAMPLES

The  $I^{131}$  sample was obtained as a fission product from Oak Ridge National Laboratory. It was thus free from large amounts of stable iodine and amenable to microwave spectroscopy. Its chemical form was NaI in a basic NaOH solution. In the final measurements, 500 millicuries of  $I^{131}$ —about four micrograms—were used. Because of the high radioactivity of the source, precautions had to be taken throughout the experiment against overexposure of harmful radiation.

The  $I^{125}$  sample was obtained by deuteron bombardment on tellurium at the Brookhaven National Laboratory. The nuclear reactions were  $Te^{124}(d,n)I^{125}$  and  $Te^{125}(d,2n)I^{125}$ . Approximately 1000 microampere hours of cyclotron bombardment were necessary to give a one-microgram yield of  $I^{125}$ . Some difficulties were

† This work was done under the auspices of the U. S. Atomic Energy Commission, and was supported in part jointly by the Signal Corps, the Office of Naval Research, and the Air Force Office of Scientific Research. Submitted in partial fulfillment of the requirements for the degree of Doctor of Philosophy in the Faculty of Pure Science, Columbia University, May, 1957.

\* Now at Hughes Aircraft Company, Culver City, California.

‡ Now at the University of Oslo, Oslo, Norway.

<sup>1</sup> L. C. Aamodt and P. C. Fletcher, Phys. Rev. **98**, 1224 (1955), and references 1-4 of that article.

<sup>2</sup> L. C. Aamodt and P. C. Fletcher, Phys. Rev. **98**, 1317 (1955), and reference 1 of that article.

<sup>3</sup> Gordy, Simmons, and Smith, Phys. Rev. **74**, 243 (1948).

<sup>4</sup> Livingston, Gilliam, and Gordy, Phys. Rev. **76**, 149 (1949).

<sup>5</sup> Livingston, Benjamin, Cox, and Gordy, Phys. Rev. **92**, 1271 (1953).

<sup>6</sup> Walchi, Livingston, and Herbert, Phys. Rev. **82**, 79 (1951).

<sup>7</sup> Koerts, Macklin, Farrelly, van Lieshout, and Wu, Phys. Rev. **98**, 1230 (1955).

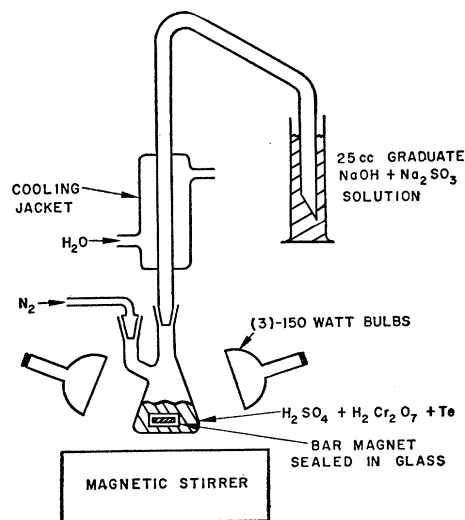


FIG. 1. Apparatus used for the separation of  $I^{125}$  from tellurium.

encountered in the construction of a tellurium target for bombardment, as solid Te is very brittle and difficult to machine and molten Te alloys very rapidly with most metals. A good Te target was constructed by coating one surface of the target holder, a 1 in.  $\times$  1 in.  $\times$  6 in. water-cooled copper block, with silver solder and grinding flat. Tellurium was then melted on top of the flat silver solder surface. The tellurium was sufficiently "soldered" to the target holder that it could be ground to any desired thickness. It was found that, owing to the poor thermal conductivity of the Te, target thicknesses greater than 0.020 inch would melt and spatter under the cyclotron beam, doing considerable damage to the cyclotron window and causing loss of  $I^{125}$  sample. When sufficient time had elapsed after the bombardment to allow short-lived radiation to die out, the tellurium was then chipped from the target holder with a hammer and chisel.

#### CHEMISTRY

The chemical synthesis of  $I^{125}$  and  $I^{131}$  into  $CH_3I$  was the same. However, the  $I^{125}$  had to be first separated from the tellurium of the target before  $CH_3I$  synthesis could begin. This separation<sup>8</sup> and synthesis of  $CH_3I^{125}$  will first be described in detail and adaptations of this procedure for the  $CH_3I^{131}$  synthesis will only be mentioned.

The  $I^{125}$  enriched tellurium chips, obtained as described above, were placed in a sulfuric and chromic acid solution, 20 cc of 18*N* sulfuric acid and 4-g anhydrous chromic acid for each gram of tellurium chips. Fifty micrograms of  $I^{127}$  were then added as carrier since the subsequent chemistry could not be done in one microgram quantities. The solution was then

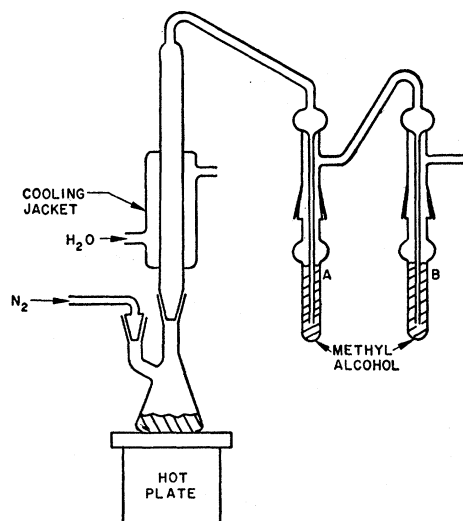


FIG. 2. Apparatus used for the concentration of iodine to 1.0 cc.

<sup>8</sup> The separation of  $I_2$  from Te follows partly a method described by K. Tangbøl and U. Blix, *Jehor Report No. 18, 1953* (unpublished).

heated by means of three 150-watt floodlights and stirred by means of a magnetic stirrer as shown in Fig. 1. In the figure, the water-cooling is initially going and the nitrogen is turned off. Both the tellurium and the iodine were thus brought to soluble oxidized states. When the tellurium was completely dissolved, the solution was cooled and anhydrous oxalic acid added, 2.36 g for each gram of tellurium chips used initially. The solution was again heated very slowly. The heat of reaction of the oxalic acid with the chromic and sulfuric acids was sufficient to keep the reaction going after it was once started and would even cause the solution to boil over if extreme care was not taken. Much  $CO_2$  was given off in this step and would carry substantial amounts of radioactive iodine away with it. Therefore the  $CO_2$  was washed with a 0.05*N* solution of  $Na_2SO_3$  and  $NaOH$ . When the reaction with oxalic acid had gone to completion, the iodine was partially in a gaseous state. The cooling water was then turned off and  $N_2$  flowed slowly over the solution. The gaseous iodine was thus carried over to the sodium sulfite solution. When no further iodine seemed to come over, the solution was cooled and 50 micrograms of  $I^{127}$  were again added and the heating and nitrogen flow repeated. Approximately 99% of the original amount of the radioactive iodine could be obtained in the sodium sulfite solution by this method.

Since some  $H_2SO_4$  fumes and other gaseous impurities came over with the iodine, and since it was necessary to concentrate the iodine into a 0.05-cc solution in order to achieve a quantitative precipitation of  $I_2$  as  $PdI_2$ , a second distillation was performed with the apparatus as shown in Fig. 2. The sodium sulfite solution obtained from the first step above was oxidized with 4-cc concentrated nitric acid and the whole solution heated with a hot plate. The iodine came off as a gas, was swept through the system with the  $N_2$ , and washed twice with 1 cc of methyl alcohol. A slight yellow coloring was seen in the first solution due to the iodine in the alcohol. (The cooling water is left on during the complete process.) The sulfite and nitric acid solution is cooled and 50 micrograms of  $I^{127}$  are added again. The process is repeated until 90–95% of the iodine is in the alcohol solutions, 70–90% in the first alcohol solution depending upon the length of time and speed of the flow of the nitrogen. The efficiency of this step can be somewhat increased by the addition of 0.2*N*  $SeO_2$  solution but this also increases the danger of impurities. The iodine is again reduced to  $NaI$  by the addition of 0.2 cc of 0.01*N*  $NaHSO_3$ , removing the yellow iodine color. Further concentration was then accomplished by the use of the apparatus in Fig. 3. The alcohol solution is heated at its surface by a nichrome filament which is manually moved down the glass tube as water is vaporized and the surface of the solution goes down. A thin capillary is inserted down the glass tube, the other end of which is attached to an aspirator, to carry away the vaporized water. As the surface level of the

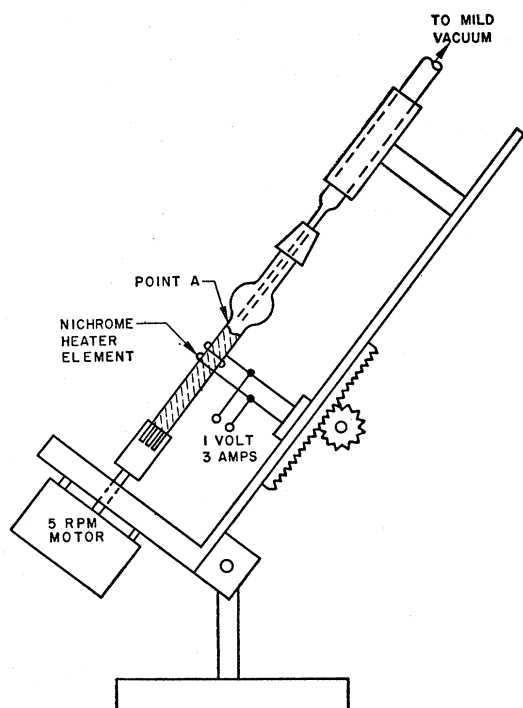


Fig. 3. Apparatus used for the concentration of NaI to 0.05 cc.

solution moves down the tube, the aspirator is periodically turned off so that the vaporized solution will condense into droplets on the sides of the glass tube and run back into the solution, thereby washing the sides of the glass tube. The tube is rotated by a clock motor at 5 rpm so that all sides of the tube are washed equally well. This process is continued until there is roughly 0.05 cc of solution left in the tube. The iodine is then precipitated by the addition of palladium chloride,  $\text{PdCl}_2$ . The precipitated  $\text{PdI}_2$  was warmed to form large particles, centrifuged, and washed twice with 0.2 cc of distilled water to remove any excess  $\text{PdCl}_2$ , the liquid being removed each time with a long, thin eye dropper. About 5% of the iodine is left in the solution and is lost. The precipitate was then dried in an oven at  $100^\circ\text{C}$  for several hours, and attached to the apparatus in Fig. 4(a) by breaking the tube in Fig. 3 at the point A and fusing it to the glass T-tube of Fig. 4(a) at point B. White phosphorus and methyl alcohol were then added in roughly stoichiometric amounts (see subsections below) and the system was then pumped out to  $10^{-6}$  mm of mercury. The tube was then sealed with an oxygen flame at point C of Fig. 4(a) while still pumping, the alcohol and phosphorus being frozen by liquid nitrogen to keep them in the capillary. The  $\text{PdI}_2$  was then decomposed by heating to  $350^\circ\text{C}$ , the iodine thus released being transferred to the capillary. However about 5% remains behind at this stage due to impurities. The capillary was then sealed off at point D of Fig. 4(a) with an oxygen torch. The iodine is then reacted by vaporizing the white phosphorus with a

gentle flame (about  $150^\circ\text{C}$ ) to make methyl iodide. The methyl iodide is admitted to the wave guide by means of the breaking tube of Fig. 4(b). The capillary tube of Fig. 4(a) is completely detached with an oxygen torch and placed in the T-tube of Fig. 4(b), with the fine tip towards the bottom. This T-tube is attached to the wave guide and pumped out. A current of 10–20 amperes is sent through the coil, thus breaking the tip of the capillary and admitting the methyl iodide to the wave guide.

(a) Alcohol was admitted after the vessels in Fig. 4(a) were pumped out by admitting a given volume at a known pressure, say 1 cc at 17 mm pressure to give one micromole.

(b) The phosphorus was added by filling capillary tubing with the white phosphorus and then cutting the tubing to the desired length. Capillary tubing of 0.05 mm can easily be drawn from 0.5 mm commercial capillary tubing. The capillary tubes can be filled by use of the T-tube in Fig. 4(c). Red phosphorus is placed at one end of the T-tube as shown and the T-tube is then evacuated. When the red phosphorus is heated droplets of white phosphorus are formed along the sides of the horizontal tube. These are driven across the tube with a flame until a large enough droplet is formed in the boss below the capillary to be filled. This then fills by capillary action. The capillary is then removed and the ends may be sealed until used. Two micromoles of phosphorus were added to the iodine to insure a complete reaction.

The  $\text{I}^{131}$  chemistry is identical with that above, omitting the initial separation with tellurium. In addition, the selenium buffer solution of the second distillation was used only with the  $\text{I}^{125}$  chemistry.

The radioactive iodine was easily followed with the aid of survey meters. All efficiencies were obtained by placing the survey meters at judicious points in each process and reading them before and after the process had been completed. The efficiencies are defined as the yield of radioactivity after the process, divided by radioactivity before the process began under similar conditions. The over-all efficiency of the process was better than 80%.

#### EXPERIMENTAL APPARATUS

Since only small amounts of samples were available, a high-sensitivity spectrometer was necessary. A conventional Stark spectrometer<sup>9</sup> with microwave frequencies being swept at about one Mc/sec per minute. This slow sweep-speed allows an increase in sensitivity.<sup>10</sup> The sensitivity was measured by observations on  $\text{CH}_3\text{I}^{127}$  vibrational lines,<sup>10</sup> which were quite abundant throughout the region where the  $\text{I}^{125}$  and  $\text{I}^{131}$  lines were expected. From these observations, the minimum observable absorption was about  $7 \times 10^{-10} \text{ cm}^{-1}$ .

<sup>9</sup> W. K. Hardy and G. Silvey, *Phys. Rev.* **95**, 385 (1954).

<sup>10</sup> C. H. Townes and H. L. Schawlow, *Microwave Spectroscopy* (McGraw-Hill Book Company, Inc., New York, 1955), p. 424.

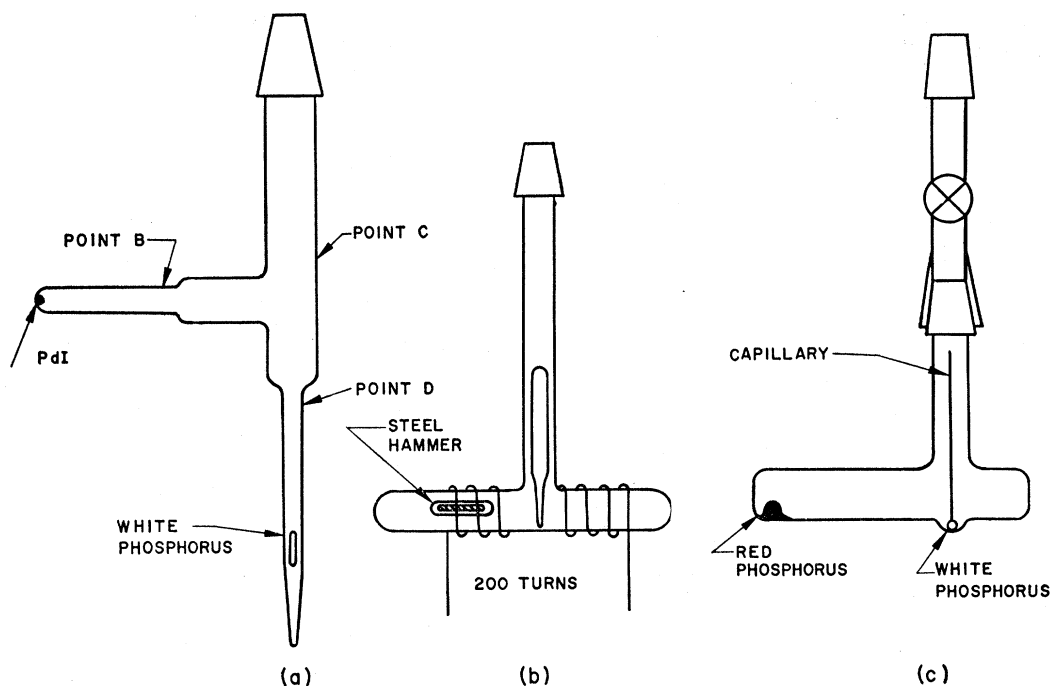


FIG. 4. Some additional apparatus. (a) Reaction vessel and allied apparatus, (b) breaking vessel, and (c) phosphorus capillary loading vessel.

The magnetic moment measurements were made with a circularly cross-sectioned wave guide to permit circularly polarized radiation, and hence, to permit the determination of the sign of the magnetic moment. The magnet was constructed of  $\frac{3}{16}$ -in. copper tubing, insulated with Fiberglas tubing and wound on a  $1\frac{1}{2}$ -in. core. Fifty-foot lengths were wound so as to give 71 turns in a  $2\frac{1}{2}$ -in. length. Sixty-five of these coils were connected in series to give about two ohms resistance. The power for the magnet was obtained from a 240-volt dc line with a grounded centertap. Each of the sixty-five coils was water cooled separately so that with 130 amperes flowing through the magnet, no temperature rise was observed. The magnetic field resulting from these coils was 1700–1800 gauss, depending upon the line voltage which was monitored by a voltmeter. The design of the magnet and wave guide which were used were similar to that used by Aamodt and Fletcher<sup>1</sup> and described in detail by Aamodt.<sup>11</sup> The large difference between the apparatus of Aamodt and that used here was that our wave guide and associated apparatus were thirteen feet in length as compared to three feet for Aamodt, thus giving an increase of four in sensitivity.

Circularly polarized radiation was obtained by slightly squeezing a circularly cross-sectioned length of wave guide at a  $45^\circ$  angle to the electric field vector inside the wave guide. This has the same effect that a quarter-wave section has in optical systems. If this "squeezed" section is placed before the absorption cell,

an attenuator at the other end can then remove one component of the circularly polarized radiation.

#### ENERGY LEVELS

The Hamiltonian,  $H$ , for a rotation molecule with one nucleus possessing a quadrupole moment in an external magnetic field may be written

$$H = H_0 + H_Q + H_M, \quad (1)$$

where  $H_0$  is the Hamiltonian for the rotational and vibrational motion,  $H_Q$  is the interaction Hamiltonian between the electric fields within the molecule and the nuclear quadrupole moment, and  $H_M$  is the interaction energy between the external applied magnetic field and the molecular and nuclear magnetic moments. The energy levels for the rotating-vibrating symmetric top molecule and the first and second-order interaction energies of the electric field with the nuclear quadrupole moment are well known.<sup>12</sup> If  $I$  is the nuclear spin,  $J$  is the molecular angular momentum,  $K$  is the component of  $J$  along the molecular axis, and  $F = I + J$ , then the first order energies in the  $IJKFM_F$  representation are

$$E_0^I + E_Q^I = \frac{\hbar^2}{4\pi^2 I_B} J(J+1) - \frac{\hbar^2}{4\pi^2} K^2 \left( \frac{1}{I_C} - \frac{1}{I_B} \right) + eqQ \left\{ \frac{3K^2}{J(J+1)} - 1 \right\} \times \left\{ \frac{\frac{3}{4}C(C+1) - I(I+1)J(J+1)}{2I(2I-1)(2J-1)(2J+3)} \right\}, \quad (2)$$

<sup>11</sup> L. C. Aamodt (to be published).

<sup>12</sup> See, for instance, reference 10, Chap. 3.

TABLE I. Observed and calculated frequencies and intensities for  $J=2 \leftarrow 1$  rotational transition of  $\text{CH}_3\text{I}^{125}$  assuming a spin of  $5/2$ ,  $eQq=2179.2$  Mc/sec and  $\nu_0=30\,053.91$  Mc/sec.

Transition $J=2 \leftarrow 1$	Frequencies, Mc/sec		Rel. intensities	
	Observed	Calculated	Observed	Calculated
3/2 3/2	30 293.1 $\pm$ 0.1	30 293.1	3	2.8
9/2 7/2	30 188.2 $\pm$ 0.1	30 188.2	10	10
9/2 7/2	30 100.0 $\pm$ 1.0	30 100.9	9	10
5/2 5/2	29 803.2 $\pm$ 1.0	29 804.1	3	5.1
7/2 5/2	29 751.2 $\pm$ 0.1	29 751.2	5	3.6

where  $C=F(F+1)-I(I+1)-J(J+1)$ ,  $I_B$  and  $I_C$  are the moments of inertia perpendicular and parallel to the molecular axis, respectively,  $e$  is the electronic charge,  $Q$  is the quadrupole moment of the nucleus, and  $q$  is the derivative of the electric field along the axis, or  $\partial^2 V/\partial z^2$ . Assuming an angular momentum transition  $J=2 \leftarrow 1$ , quadrupole patterns for spins at  $\frac{3}{2}$ ,  $\frac{5}{2}$ ,  $\frac{7}{2}$ , and  $9/2$  have been calculated. These are shown, together with the observed lines of  $\text{I}^{125}$  in Fig. 5. Second-order quadrupole interaction corrections have not been included but are not sufficiently large to change the figure greatly.

In an  $IJKFM_F$  representation the magnetic interaction Hamiltonian has off-diagonal element connecting states of the same  $M_F$  but  $F$  changes by 1. Coester<sup>13</sup> gives the interaction energy of a symmetric top with hyperfine structure in an external magnetic field to second order as

$$E_{M^1} = \mu_0 H M_F \left\{ g_I \left( \frac{I(I+1) - J(J+1) + F(F+1)}{2F(F+1)} \right) + g_J \left( \frac{J(J+1) - I(I+1) + F(F+1)}{2F(F+1)} \right) \right\}, \quad (3)$$

$$E_{M^2} = \frac{(\mu_0 H)^2}{eQq} \frac{(g_I - g_J)^2}{\{3K^2/[J(J+1)] - 1\}} \left\{ \frac{R(F)(F^2 - M_F^2)}{G(F) - G(F-1)} + \frac{R(F+1)(F+1)^2 - M_F^2}{G(F) - G(F+1)} \right\},$$

where

$$R(F) = \frac{[F^2 - (I-J)^2][I(I+1) - J(J+1) - F^2]}{4F^2(2F-1)(2F+1)},$$

$$G(F) = \frac{\frac{3}{2}C(C+1) - I(I+1)J(J+1)}{(2J+3)(2J-1)(2I)(2I-1)},$$

$C$  is the same as in Eq. (1),  $\mu_0$  is the nuclear magneton,  $H$  is the magnetic field, and  $g_I$  and  $g_J$  are the nuclear and molecular  $g$  factors, respectively. Exact diagonalization of the  $H_0$  and  $H_M$  energy matrix, similar to that done by Aamodt and Fletcher,<sup>2</sup> indicates that, to the accuracy of this experiment, the above second-order corrections are sufficient.

<sup>13</sup> F. Coester, Phys. Rev. **77**, 454 (1950).

### OBSERVED LINES OF $\text{CH}_3\text{I}^{125}$

Five lines of the  $J=2 \leftarrow 1$  hyperfine pattern of  $\text{CH}_3\text{I}^{125}$  have been seen and are plotted in Fig. 5. Unfortunately, accurate measurements were obtained on only three of these lines. The measured and calculated frequencies together with the observed and calculated intensities are given in Table I. The calculated frequencies were obtained by assuming a spin of  $\frac{5}{2}$ , a quadrupole coupling constant of 2179.2 Mc/sec and a rotational frequency,  $\nu_0$ , equal to 30 053.91 Mc/sec. Using the value of the quadrupole moment of  $\text{I}^{127}$  given by Jaccarino, King, Satten, and Stroke,<sup>14</sup> together with its quadrupole coupling constant,<sup>3</sup> the quadrupole moment of  $\text{I}^{125}$  is found to be  $-0.66 \times 10^{-24}$  cm<sup>2</sup>. This spin and quadrupole moment would indicate a predominantly  $d_{3/2}$  ground state configuration for  $\text{I}^{125}$ . Rough measurements on the Zeeman splitting of the  $F=9/2 \leftarrow 7/2$ ,  $J=2 \leftarrow 1$  hyperfine line give  $\mu(\text{I}^{125}) = 3.0 \pm 1.0$  nm and would tend to indicate that  $\text{I}^{125}$  has a ground state similar to that of  $\text{I}^{127}$ .

### ZEEMAN SPLITTING IN $\text{CH}_3\text{I}^{131}$

The Zeeman components of the  $F=9/2 \leftarrow 9/2$  hyperfine line of the  $J=2 \leftarrow 1$  rotational transition are

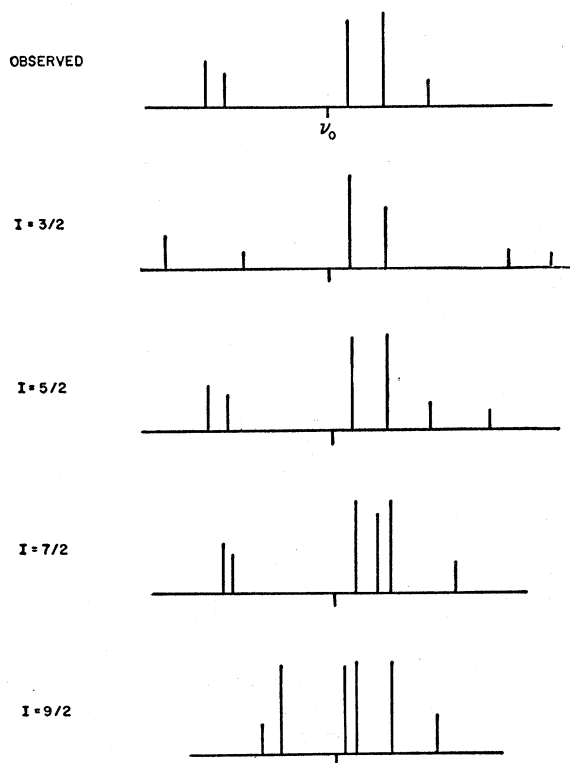


FIG. 5. Comparison of the quadrupole patterns of the  $J=2 \leftarrow 1$  rotational transition for spins of  $3/2$ ,  $5/2$ ,  $7/2$ , and  $9/2$ . The observed lines are included for comparison.

<sup>14</sup> Jaccarino, King, Satten, and Stroke, Phys. Rev. **94**, 1798 (1954).

shown in Fig. 6. Second-order corrections are included in the frequencies but not in the intensities, since this would not alter the picture appreciably. Also, measurements on  $\text{CH}_3\text{I}^{127}$  indicate that the molecular  $g$  factor,  $g_J$ , equals zero to the accuracy of these measurements. Since the lowest mode in a circular wave guide is a  $TE$  mode, and the magnetic field is axial along the wave guide, the electric and magnetic fields should be perpendicular and only  $\Delta M_F = \pm 1$  should be excited. However, because of reflections and imperfections in the wave guide, the next highest mode, a  $TM$  mode, is excited. The electric and magnetic vectors are no longer perpendicular and the  $\Delta M_F = 0$  transitions are permitted, their intensity being dependent upon the reflections in the wave guide. Change in polarization due to changes in the "quarter-wave" section of wave guide gives a change in the relative amplitude of  $\Delta M_F = +1$  and  $\Delta M_F = -1$  components. Three different ratios of relative amplitudes of  $\Delta M_F = +1$ :  $\Delta M_F = -1$ :  $\Delta M_F = 0$  are used to compute line intensities. These are given in Fig. 7 together with their envelope and the experimentally observed traces. A value for  $\mu_0 g_I H$  of  $0.96 \pm 0.05$  Mc/sec was used throughout the theoretical calculations, the resulting envelopes fitting quantitatively all three peaks ( $\Delta M_F = \pm 1, 0$ ). From similar tests on  $\text{I}^{127}$ , the sign of the magnetic moment was determined to be the same as the magnetic moment of  $\text{I}^{127}$ .

The magnetic field was determined by measurements of the Zeeman splitting of the hyperfine lines of the  $J=2 \leftarrow 1$  rotational pattern of  $\text{CH}_3\text{I}^{127}$ . The average of the results of splitting of three lines, the  $F=9/2 \leftarrow \frac{5}{2}$ , the  $F=\frac{5}{2} \leftarrow \frac{5}{2}$  and the  $F=\frac{1}{2} \leftarrow \frac{3}{2}$  gave a value for  $\mu_0 g_I H$  for  $\text{I}^{127}$  of  $1.48 \pm 0.01$  Mc/sec (normalized to the same value of magnet current for which the value of  $\mu_0 g_I H$  is quoted above for  $\text{I}^{131}$ ). Using the ratio of  $g$  factors thus obtained, remembering the difference of spins and using the value of the magnetic moment of  $\text{I}^{127}$  given by Walchi, Livingston, and Herbert<sup>6</sup> of  $\mu(\text{I}^{127}) = 2.8090 \pm 0.0004$  nuclear magnetons, we find a

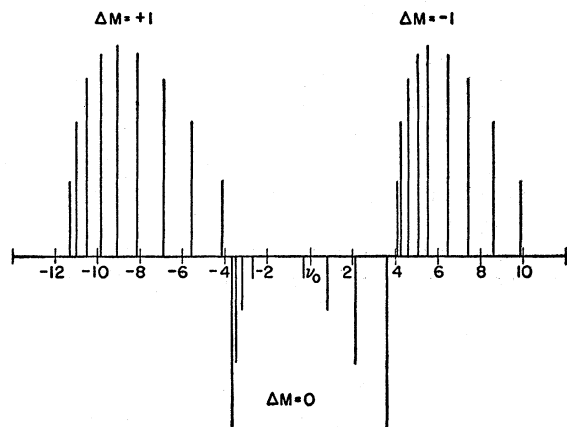


FIG. 6. Magnetic hyperfine components for the  $F=9/2 \leftarrow 9/2$ ,  $J=2 \leftarrow 1$  rotational transition assuming  $\mu_0 g_I H = 1.00$  Mc/sec.

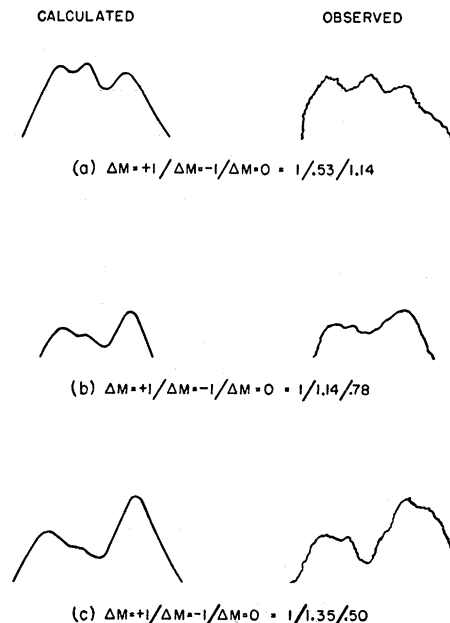


FIG. 7. Calculated and observed Zeeman splitting of  $F=9/2 \leftarrow 9/2$ ,  $J=2 \leftarrow 1$  hyperfine line of  $\text{CH}_3\text{I}^{131}$ .

value for the magnetic moment of  $\text{I}^{131}$  of  $\mu = 2.56 \pm 0.12$  nuclear magnetons. This would indicate that  $\text{I}^{131}$  has a ground state similar to that of  $\text{I}^{129}$  which has a magnetic moment of  $\mu(\text{I}^{129}) = \pm 2.61$  nuclear magnetons.

Comparative data for  $\text{I}^{125}$ ,  $\text{I}^{127}$ ,  $\text{I}^{129}$ , and  $\text{I}^{131}$  are listed in Table II.

#### DISCUSSION

According to the single-particle model proposed by Mayer<sup>15</sup> and by Haxel *et al.*,<sup>16</sup> the spin and magnetic moment of a nucleus is determined by the last unpaired nucleons, the quadrupole moment by the nucleons in unfilled shells. It is well known that the single-particle shell model gives quadrupole moments much smaller than observed experimentally, and that distortion of the closed shells actually contributes importantly to the large size of nuclear quadrupole moments. Bohr and Mottelson<sup>17</sup> use a model in which the nuclear particles of the core, i.e., all particles excluding the unpaired ones, undergo a collective type of vibration. The quadrupole moments calculated on the basis of this model agree qualitatively with measured values. Following the Bohr-Mottelson model, Nilsson<sup>18</sup> calculated the energy levels and wave functions by adopting a simple single-particle Hamiltonian of the form

$$H = -\frac{\hbar^2}{2M} \nabla^2 + \frac{M}{2} \{ \omega_x^2 x^2 + \omega_y^2 y^2 + \omega_z^2 z^2 \} + C \mathbf{l} \cdot \mathbf{s} + D \mathbf{l}^2, \quad (4)$$

<sup>15</sup> M. Goepfert-Mayer, Phys. Rev. **78**, 16 (1950).

<sup>16</sup> Haxel, Jensen, and Suess, Phys. Rev. **75**, 1766 (1949).

<sup>17</sup> A. Bohr and B. Mottelson, Kgl. Danske Videnskab. Selskab, Mat.-fys. Medd. **27**, 16 (1953).

<sup>18</sup> S. G. Nilsson, Kgl. Danske Videnskab. Selskab, Mat.-fys. Medd. **29**, 16 (1955).

TABLE II. Comparative data for  $I^{125}$ ,  $I^{127}$ ,  $I^{129}$ , and  $I^{131}$ .

	$I^{125}$	$I^{127}$	$I^{129}$	$I^{131}$
Spin	5/2	5/2	7/2	7/2
Quadrupole coupling constant, Mc/sec	2179	1934	1422	973
Quadrupole moment, $\text{cm}^2 \times 10^{24}$	-0.66	-0.59	-0.43	-0.29
Magnetic moment, nm	$3.0 \pm 1.0$	$2.8990 \pm 0.0004$	$2.6173 \pm 0.0003$	$2.56 \pm 0.13$

where  $x'$ ,  $y'$ , and  $z'$  refer to the coordinates of the particle in a coordinate system fixed in the nucleus. This has the form of a spherical harmonic oscillator potential with spin-orbit coupling. Nilsson then confines himself to cylindrical symmetry of the core such that

$$\begin{aligned}\omega_x^2 &= \omega_y^2 = \omega_0^2(1 + \frac{2}{3}\delta), \\ \omega_z^2 &= \omega_0^2(1 - \frac{4}{3}\delta),\end{aligned}\quad (5)$$

where  $\delta$  is a measure of the deformation of the core. In terms of this deformation parameter, the quadrupole moment may be written,

$$Q = 0.82R_Z^2\delta(1 + \frac{2}{3}\delta) \frac{I(2I-1)}{(I+1)(2I+3)}, \quad (6)$$

where  $R_Z$  is the average radius of the core given approximately by  $1.2 \times 10^{-13} A^{\frac{1}{3}}$  cm.

Deformation parameters for the iodine nuclei have been calculated on the basis of Eq. (6) and plotted in Fig. 8. It is evident from this figure that as the closed neutron shell of 82 is approached, the deformation of the nucleus decreases. The deformation parameter of  $\text{Pr}^{141}$ , with a completely closed shell of 82 neutrons, is plotted on the same diagram and shows a further marked decrease over values for the unfilled neutron shell. Such a result is expected qualitatively because of the high stability of the spherical closed shell of neutrons.

The fourth shell closes with 50 nucleons and levels within the fifth shell should occur, in the absence of any interaction with the core, in the order  $g_{7/2}$ ,  $d_{5/2}$ ,  $d_{3/2}$ ,  $s_{1/2}$ , and  $h_{11/2}$ . Thus iodine, with 53 protons, three outside the closed shell, should have a  $g_{7/2}$  configuration for its ground state. With the introduction of the

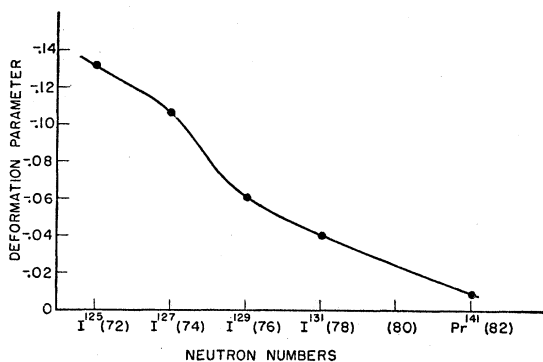


FIG. 8. Deformation parameter vs neutron number for iodine and  $\text{Pr}^{141}$ .

deformation of the core and coupling of the single particle to this deformed core, considerable deviation from the above ordering may be obtained. Nilsson tabulates the energy levels as a function of the deformation parameter. Unfortunately, he has chosen his constants  $C$  and  $D$  of Eq. (4) so that the  $d_{5/2}$  level falls below the  $g_{7/2}$  level for a spherical core, i.e., for  $\delta=0$ . Figure 8 indicates the opposite to be true—that as the core approaches sphericity, the  $g_{7/2}$  level becomes more stable.  $\text{Pr}^{141}$  has a spin  $\frac{5}{2}$ , even though it had a nearly spherical core, because the  $g_{7/2}$  level for protons has been filled. Furthermore, Nilsson's calculation indicates that with increasing deformation in the direction of negative quadrupole moments, the energy of the  $g_{7/2}$  level decreases with respect to that of the  $d_{5/2}$  level. This is just the reverse of what is observed. However, it must be realized that the nuclei measured differ from each other not only in the amount of deformation, but to a small extent in the nuclear size and in the neutron-proton ratio. Thus the greater stability of the  $g_{7/2}$  level with the addition of neutrons may not be due to the change in deformation alone, which is the only variation allowed in Nilsson's calculation, but to the increased nuclear size as neutron-proton ratio.

It is interesting to note that the change of spin from  $\frac{5}{2}$  to  $\frac{7}{2}$  as a closed neutron shell is approached is not peculiar to iodine. Table III lists the spins and magnetic moments for other nuclei in this region. Both Sb and Cs show the same behavior. The change of spins is indicated by the dashed line in the table. The arrows in the table indicate the stable isotopes of the element. The change of spin from  $\frac{7}{2}$  to  $\frac{5}{2}$  seems to occur characteristically near the isotope of maximum stability. One might predict empirically on the basis of the table that the spin of  $\text{La}^{137}$  is  $\frac{5}{2}$ .

It is also seen from Table III that the magnetic moments of nuclei with the same spin but cores of different neutrons, protons, and quadrupole moments, are nearly equal. Thus, nuclei with spins  $\frac{5}{2}$  have magnetic moments about 3.2 nm and nuclei with spins  $\frac{7}{2}$  have magnetic moments about 2.7 nm. This is in qualitative agreement with the Bohr-Mottelson model since the effect of the core on the magnetic moment comes in only through the coupling of the core to the unpaired particles which are primarily responsible for the magnetic moments. The magnetic moment of  $\text{Pr}^{141}$ , which has only weak coupling from the core to the unpaired particle, of 3.8 nm approaches more closely than the other cases to the single-particle (Schmidt) limit of 4.8 nm.

TABLE III. Comparison of magnetic moment in nm and spin for elements with neutrons near closed shell V (82) and unfilled  $g_{7/2}$  proton subshell. All values are found from nuclear magnetic resonance methods except where errors are indicated.<sup>a, b</sup>

Neutrons \ Protons	51 (Sb)		53 (I)		55 (Cs)		57 (La)		59 (Pr)	
	<i>I</i>	$\mu$	<i>I</i>	$\mu$	<i>I</i>	$\mu$	<i>I</i>	$\mu$	<i>I</i>	$\mu$
70	→5/2	3.34								
72	→7/2	2.53	5/2	3.0 ± 1.0						
74			→ 5/2	2.81						
76			7/2	2.61	5/2	3.48				
78			7/2	2.56 ± 0.12	→7/2	2.56				
80					7/2	2.71				
82					7/2	2.82	→7/2	2.76	→ 5/2	3.8

<sup>a</sup> Arrows indicate the abundant stable nuclei.  
<sup>b</sup> Dashed line indicates transition from spin 5/2 to spin 7/2.

CONCLUSIONS

It is seen from the foregoing that the general features of the nuclear moments of iodine and iodine-like nuclei are in agreement with the single-particle model and its modifications. However, there is lack of detailed agreement with the fairly comprehensive treatment of Nilsson of deformed nuclei. Furthermore, more accurate measurements are needed to test empirical rules such as that of Bohr<sup>19</sup> concerning the relationship of the change of the magnetic moment and the quadrupole

moment with the addition of two neutrons to nuclei with identical spins. A quite systematic change from spins of  $\frac{7}{2}$  to spins of  $\frac{5}{2}$  can be seen at the point of the most stable nucleus of the isotopic series of iodine and other neighboring elements.

ACKNOWLEDGMENTS

The authors are grateful to Dr. C. H. Townes for his suggestion of this research and his direction of it. It is a pleasure to acknowledge also the helpful assistance of members of the staff of the Columbia Radiation Laboratory throughout the project.

<sup>19</sup> A. Bohr, Phys. Rev. **81**, 134 (1951).